galaxies

MDPI

Article

A "Wonderful" Reference Dataset of Mira Variables

Dana K. Baylis-Aguirre [1,*], Michelle J. Creech-Eakman [1,*] and Gerard T. van Belle [2,*]

[1] Physics Department, New Mexico Tech, Socorro, NM 87801, USA
[2] Lowell Observatory, Flagstaff, AZ 86001, USA
* Correspondence: mailto:dana.baylisaguirre@nmt.edu (D.K.B.-A.); michelle.creecheakman@nmt.edu (M.J.C.-E.); gerard@lowell.edu (G.T.v.B.)

Abstract: The conditions in Mira variable atmospheres make them wonderful laboratories to study a variety of stellar physics such as molecule–grain formation, dust production, shock chemistry, stellar winds, mass loss, opacity-driven pulsation, and shocks. We were awarded an NSF grant to analyze over a decade of synoptic observations from the Palomar Testbed Interferometer (PTI) of 106 Miras to curate a *Mira Reference Dataset*. The Miras included in this dataset include M-types, S-types, and C-types, and span a wide range of pulsation periods. PTI measured K-band angular sizes that when combined with a distance allow us to directly determine fundamental stellar parameters such as effective temperature, radial size, and bolometric flux. Supplementing observations with interferometric measurements of the stars opens the Mira laboratory to a wealth of different experiments. We provide two case studies to serve as examples of the power of the *Mira Reference Dataset*. The first case study describes combining PTI measurements with Spitzer IRS spectra of M-type Miras, which allowed us to fully characterize CO_2 gas in their atmospheres. The second case study examines how PTI narrow-band data can be used to study phase-dependent pulsation effects on the stellar atmosphere. We provide a list of all the Miras (with coordinates) included in the set for anyone who would like to add them to their observing programs. All the data we produce and collate for this *Mira Reference Dataset* will be hosted and curated on a website open to the public so that other researchers and citizen scientists can participate in expanding the utility and body of knowledge on this set of "wonderful" stars.

Keywords: Mira variables; Mira Reference Dataset; techniques: (long-baseline interferometry, high-angular resolution); instrument: Palomar Testbed Interferometer (PTI); stars: fundamental parameters (angular diameters, radii, temperatures)

check for updates

Citation: Baylis-Aguirre, D.K.; Creech-Eakman, M.J.; van Belle, G.T. A "Wonderful" Reference Dataset of Mira Variables. *Galaxies* **2024**, *12*, 72. https://doi.org/10.3390/galaxies12060072

Academic Editor: Dominic Bowman

Received: 15 September 2024
Revised: 27 October 2024
Accepted: 29 October 2024
Published: 31 October 2024

Copyright: © 2024 by the authors. Licensee MDPI, Basel, Switzerland. This article is an open access article distributed under the terms and conditions of the Creative Commons Attribution (CC BY) license (https://creativecommons.org/licenses/by/4.0/).

1. Introduction

Asymptotic giant branch (AGB) stars are highly evolved low-to-intermediate mass (∼0.8–8 $M_\odot$) stars characterized internally by alternate shell burning atop a degenerate C/O core, and externally by their highly extended, and chemically complex circumstellar environments (CSEs). The dynamic nature of pulsating AGB atmospheres creates distinct asymmetries that can arise from convective spots, non-radial pulsation, episodic mass loss, etc. [1]. Cool photospheric temperatures (2500–3500 K) combined with high mass loss rates (10^{-8}–10^{-4} $M_\odot$/yr) make AGB stars some of the most prolific dust and molecule factories in the Universe, and foremost sources of chemical enrichment of the interstellar medium (ISM). For contemporary galaxies, AGB stars are the primary producers of interstellar dust, and at cosmological distances, they compete with dust produced in supernovae ejecta [2].

Mira variables are a subset of AGB stars characterized by large amplitude pulsations ($\Delta m_V > 2.5$) and regular periods longer than 100 days. Miras have gentle (∼10 km/s) but relentless winds that combine with their regular pulsations to launch material into the surrounding CSE at dramatic mass loss rates. Ongoing theoretical studies [3] indicate that as Miras reach their final stages of evolution, they approach a "death-cliff", where the mass loss reaches a state such that the star essentially disintegrates as it evolves toward the terminal planetary nebula stage.

Regular pulsation and cool atmospheres make Miras prolific factories of molecules and dust, creating chemically rich circumstellar environments (CSEs) that expand around each star. More than 100 molecules (roughly half of the total interstellar species) and 15 dust species have been detected in AGB outflows [4,5]. The chemical composition of an individual Mira's CSE depends on the C/O ratio. More massive Miras will undergo additional thermal pulses and subsequent convective overshoot events that dredge up enough carbon to alter their chemical composition over time; the chemical sub-class evolution moves from oxygen-rich (M-types, C/O <1), to "intermediate" (S-types, C/O ∼1), and carbon-rich (C-type, C/O > 1) as third dredge-up activity alters the stellar surface composition over time [6,7]. For M-type Miras, the majority of carbon is quickly bound in CO molecules that form adjacent to the photosphere, although the existence of certain molecules like CO_2, and HCN indicate that shock chemistry plays a significant role in shaping the molecular environments of these stars [8]. Other typical molecules found in M-type atmospheres include VO, SiO, H_2O, TiO, and SO_2. S-type Miras will show a mix of oxygen and carbon-rich species and complex intermediate chemistry [9,10]. C-type Miras are characterized by "sooty" species including CN, C_2, HCN, C_2H_2, polycyclic aromatic hydrocarbons (PAHs) [11], and fullerenes (C_{60} and C_{70}) [12].

Despite substantial efforts toward understanding the physical conditions driving molecule formation, dust production, and mass loss in AGB and Mira atmospheres [7,13], many of the nuances remain poorly understood. Mira atmospheres provide the perfect laboratory to study time-dependent behaviors within their CSEs to further advance our understanding of how pulsation affects mass loss processes. However, such advancements will require phase-dependent, multi-wavelength observations, and time-series data analysis on a set of *individual* Miras to unveil pulsation-driven or shock-driven conditions. To directly address this need, our working group is currently building a time-dependent, **observational** *Reference Dataset* for ∼100 Miras, which we will provide to the astrophysical community to utilize in new theoretical studies and modeling efforts in the coming years.

1.1. Fundamental Stellar Properties

A star's evolutionary state is governed by five fundamental physical properties: luminosity, (L), effective temperature (T_{eff}), radius ($R_\star$), mass (M), and chemical composition (Z). Directly observing or measuring any of these five properties is exceedingly difficult for most stars. Miras, however, offer some distinct advantages for determining their fundamental properties. Typical Mira radii are ∼1 AU, so targets within 1 kpc exhibit angular diameters ranging from several to tens of milliarcseconds (mas), making them excellent candidates for direct angular size measurements with near-infrared interferometry. Their intrinsically bright luminosities at the H-and K-bands mean their angular diameters can be measured quickly and repeatedly with phase.

1.2. Distances

When discussing fundamental stellar parameters, the elephant in the room is, of course, distance. Miras for the monitoring program were originally selected for maximum sensitivity for the Palomar Testbed Interferometer (PTI); this required bright targets (in H-and K-bands) for overall SNR, and for each target to have angular diameters between 2–5 mas for optimum visibility measurements (i.e., targets <2 mas and >5 mas will be under- and over-resolved, respectively). This angular diameter requirement places *all* PTI targets within ∼1 kpc. Determining more precise distances to these targets from their parallax measurements is a non-trivial process. For example, Table 2 in [14] compares parallax measurements and subsequent distance estimates for 13 M-type PTI Miras observed with both Hipparcos (updated calibration [15]) and Gaia (DR2, available at the time of publication [16]). There is clearly a discrepancy between the two surveys that go beyond Gaia's updated capabilities; in the case of *R Tri*, their respective error bars do not even overlap.

Accurately determining parallaxes in AGB stars is a well-documented challenge, as shown in Refs. [17–19]. Gaia, in particular, struggles with measurements of Miras for

three primary reasons: (1) Miras are intrinsically red sources and Gaia's image parameter designation is not well-characterized for targets redder than $\nu_{\rm eff} = 1.24$ μm^{-1} [20]. (2) Miras are known variable stars, but the current astrometric pipeline uses a *fixed* color, creating systematic uncertainty as Mira's color evolves with its pulsation cycle [19,21]. (3) AGB atmospheres are characterized by complex, dynamic convective cells, e.g., [and references therein] [1] contributing to photocenter wobbles ∼10% of the stellar radius [19,22,23] (in the optical), which becomes a significant source of noise in Gaia astrometry. This noise is further amplified when we consider (2) and (3) together, because Miras have $\Delta V \geq 2.5$, with many having ΔV=6–8 across the pulsation cycle. The intrinsically higher uncertainty in the location of the star's photocenter for each measurement leads to larger error bars on the distances than we would expect to see for a non-varying star of this magnitude. Unless otherwise specified, we adopt a generic distance of 1 kpc for PTI Miras for the following discussions.

1.3. Period-Luminosity Relationship

Miras have a period-luminosity (P-L) relationship, e.g., [24,25], meaning they, like their more famous cousins, the Cepheids, can be utilized as standard candles to provide rungs on the distance scale ladder [26]. However, two factors provide Miras a distinct observational advantage over Cepheids to measure rungs on this local distance ladder. (1) Mira progenitors are typically lower mass than Cepheids [27], expanding the types of galaxies in which they will be found [28]. (2) Miras are brighter than Cepheids at IR wavelengths [29], which are superior to optical bands for constraining P-L relationships because of reduced extinction effects [24]. These observational advantages make it critical to advance the *calibration* of Mira P-L relationships, which requires understanding their pulsation mode and how the physical *sizes* and *shapes* of the atmosphere evolve through a pulsation cycle.

Considerable effort has been devoted to determining the pulsation modes of Miras based on P-L relationships (e.g., [30–32]) for different populations of long-period variables. Some researchers in the community [30] argue that Miras all pulsate in the fundamental mode, a conclusion supported by population synthesis models and statistical analyses of long-period variables in the Large Magellanic Cloud. These efforts rely on analyzing P-L relationships to determine the pulsation models; however, these results are based on large statistical samples and have yet to be tested against individual Miras. Recent modeling efforts [3] indicate that pulsating AGB stars with intermediate periods (∼100–250 d) can be fundamental *or* overtone pulsators, and that pulsation in *either* mode may immediately precede the Mira going over the "death cliff" of catastrophic mass loss. For an individual Mira, determining the pulsation mode requires precise knowledge of its mass. We adopt an alternative course of action to improve the P-L relationship by using interferometry to resolve the stellar disk and sample at multiple phase points to directly measure how the size (ΔR/R) and shape of the star respond to the pulsation [33].

2. Insights from Long-Baseline Infrared Interferometry

For the past ∼40 years, interferometric techniques have been powerful tools to *directly* measure and study Mira variables' dynamic atmospheres, CSEs, and the pulsation-driven relationships of measurable quantities, e.g., [34,35]. Angular diameters (θ) measured at 2.2 μm can serve as proxies for the Rosseland mean photospheric diameter, as noted by [17], thus allowing us to study the relationship between the pulsating photosphere and the surrounding atmospheric layers.

Harvard CfA's Infrared Optical Telescope Array (IOTA) facility recorded Mira diameters within the range of 350–600 $R_\odot$; astonishingly, these diameters vary in size by 10–30% across the pulsation cycle [6,17,36]. Additionally, ref. [37] showed that in the near-IR, **75%** of all well-resolved AGB stars showed asymmetry, and **100%** of their M-type Miras showed asymmetry; ref. [38] reported similar levels of asymmetry in C-types using PTI. Departure from spherical symmetry can result from several phenomena, including mass loss events,

photospheric activity such as spots, non-radial pulsation modes, "patchy" molecular layers, spin-up from exoplanet ingestion, and any combination thereof. These phenomena create asymmetries in either the surface brightness of the star or by making its shape more oblate (or both).

The IOTA experiments also indicated that angular sizes of Miras are *wavelength dependent*, with $\theta(J) < \theta(H) < \theta(K)$ [39]. At finer steps within these broadband windows, we can start to study spectroscopic features that help explain this wavelength-dependent phenomenon. For example, within the K-band, angular sizes measured longwards of μm are systematically larger than those around ∼2.2 μm, which are typically associated with continuum emission for these stars [40]. This increase in observational size is likely an opacity effect [18], created by several ro–vibrational bands of CO that lie between 2.29 and 2.5 μm.

The Palomar Testbed Interferometer (PTI)

The Palomar Testbed Interferometer (PTI) was a near-IR long-baseline interferometer with baselines ranging from 85 to 110 meters. It operated in the H-band (1.6μm) and K-band (2.2 μm). It was located at the Palomar Observatory in San Diego, California, and was originally constructed by NASA to serve as a "testbed" of interferometric techniques for the Keck Interferometer; a detailed description is provided in Colavita et al. [41]. Three 40-cm apertures were combined pairwise to measure stellar fringe visibility on targets that ranged from 0.5 to ∼5 milliarcseconds (mas) in size and were able to resolve individual targets with angular sizes $\theta > 0.75$ mas. PTI operated nightly between 1997 and 2008 with minimal downtime. The data collected by PTI considered in our *Mira Reference Dataset* spans from 1998 to 2008, making it one of the most prolific monitoring programs for individual Mira variables to date.

The scientific goal of this extensive observational program was to study phase-dependent behavior of both wide- and narrowband angular size(s) to look for any trends across chemical sub-classes, pulsation modes, and spatial geometry. We analyzed the entire wideband dataset for these Miras and are preparing it for publication. While still only in the preliminary analysis, the more spectrally detailed, narrowband dataset is already revealing tantalizing clues to pulsation-driven effects on the atmosphere (see Section 3.2).

3. A Reference Dataset

The full sample set of PTI-monitored Miras provided in Table 1 exhibits a wide range in both chemistry and pulsation period (see Figure 1), making it statistically representative of the general population of Galactic Miras. We employ the following steps to directly extract phase-dependent T_{eff} and $R_\star$.

Table 1. List of Targets included in the *Mira Reference Dataset* with their respective coordinates (ICRS J2000), periods ([1][42]), and chemistries.

Target	RA	DEC	Period [1] (Days)	Chemistry
RW And	00 47 18.9203868696	+32 41 08.247572160	430	S
ST And	23 38 45.1330125288	+35 46 21.242761248	326.6	C
SV And	00 04 20.0747373144	+40 06 35.834145228	313	M
T And	00 22 23.1498952512	+26 59 45.746339820	281	M
TU And	00 32 22.7282685288	+26 01 45.921110808	316.8	M
X And	00 16 09.5930847264	+47 00 44.476093440	343.4	S
Y And	01 39 36.8890293264	+39 20 34.906702164	220.5	M
OW Aql	19 51 21.8844282456	+15 00 12.364210332	416.6	C
RT Aql	19 38 01.6040590464	+11 43 18.231266280	326.4	M
S Aql	20 11 37.4682590352	+15 37 14.587639716	147	M

Table 1. *Cont.*

Target	RA	DEC	Period [1] (Days)	Chemistry
SY Aql	20 07 05.4056873352	+12 57 06.224235444	359.7	M
X Aql	19 51 29.8017062424	+04 27 51.655142052	347.7	M
Z Aql	20 15 11.0411716872	−06 09 03.965069232	128.4	M
T Aqr	20 49 56.4076942032	−05 08 47.958242604	201	M
RU Ari	02 44 45.4939002600	+12 19 03.001204056	353.5	M
U Ari	03 11 03.0366056664	+14 48 00.300444804	371.1	M
RU Aur	05 40 07.8949580712	+37 38 10.677481116	463	M
V Aur	06 24 02.3342525640	+47 42 23.854783788	349	C
W Aur	05 26 54.5689577640	+36 54 11.152186740	271.3	M
X Aur	06 12 13.3836194376	+50 13 40.434769452	165.5	M
R Boo	14 37 11.5761577632	+26 44 11.656214052	233.1	M
RT Boo	15 17 14.7082315152	+36 21 33.437211804	275	M
RW CVn	13 59 33.4689506184	+37 11 50.313181560	100	M
U CVn	12 47 19.6073883768	+38 22 30.655400808	342.9	M
V CVn	13 19 27.7658321448	+45 31 37.656251760	194	M
X Del	20 54 54.1288659648	+17 38 29.901148584	285.6	M
Y Del	20 41 38.9763815280	+11 52 38.262989496	281	M
WZ Dra	16 59 49.7294536200	+52 19 04.469517552	468.4	M
R Gem	07 07 21.2705134872	+22 42 12.747215448	401.7	M
S Gem	07 43 02.5547544792	+23 26 58.140767004	369.9	S
T Gem	07 49 18.1736908200	+23 44 04.087533444	293.2	M
V Gem	07 23 09.3495183408	+13 06 04.826953476	287.8	S
VX Gem	07 12 48.9705620544	+14 36 03.716151984	274.8	M
X Gem	06 47 07.0499826432	+30 16 34.308326136	379.4	C
ZZ Gem	06 24 01.2452265672	+25 01 52.889018700	264.2	M
R Her	16 06 11.7085696296	+18 22 13.205307324	317	C
RS Her	17 21 42.3553596648	+22 55 16.040460324	318.1	M
RV Her	17 00 33.2457227280	+31 13 23.811867876	219.7	M
RZ Her	18 36 47.0163321144	+26 02 57.339469536	205.2	M
S Her	16 51 53.9188877832	+14 56 30.763623732	329.1	M
SV Her	18 26 23.0951611296	+25 01 33.145841244	307.3	M
SY Her	17 01 29.2529062944	+22 28 38.724358044	293	M
T Her	18 09 06.2110690224	+31 01 16.203768384	116.9	M
W Her	16 35 12.3157321728	+37 20 43.017169884	164.9	M
SS Cas	00 09 36.5268503344	+51 34 00.886929949	280.3	M
TT Cas	00 10 09.1456062240	+54 52 34.390697952	140.6	M
U Cas	00 46 21.3733079520	+48 14 39.865023492	396	M
V Cas	23 11 40.7202756960	+59 41 58.979830092	278.9	S
WY Cas	23 58 01.3064089800	+56 29 13.475449716	230.6	M
R Cet	02 26 02.3168041392	−00 10 41.813680476	481.5	S
Z Cet	01 06 45.1233876504	−01 28 53.132348388	166.2	M
R Com	12 04 15.1986066432	+18 46 56.767920564	184.8	M
R CMi	07 08 42.6121220544	+10 01 26.458092084	362.8	M
U CMi	07 41 20.0306710320	+08 22 49.111425372	340	C
V CMi	07 06 58.8155828616	+08 52 37.109136144	412.1	M
V Cnc	08 21 42.8232235656	+17 17 06.474585588	366.3	M
V CrB	15 49 31.3121978280	+39 34 17.892629256	269.7	S
X CrB	15 48 53.5259660688	+36 14 52.594027944	357.6	C
R Cyg	19 36 49.3579856496	+50 11 59.727536988	241.2	M
RT Cyg	19 43 37.7664119520	+48 46 41.333575404	426.5	S
LX Cyg	21 55 57.0262652688	+48 20 52.522680876	190.3	M
U Cyg	20 19 36.5946317760	+47 53 39.096681828	465.3	C
UX Cyg	20 55 05.5117404456	+30 24 52.015482108	463.2	C
WX Cyg	20 18 33.2742966672	+37 26 59.080236792	565	M
Z Cyg	20 01 27.5075704056	+50 02 32.634937212	410.5	C
RV Peg	22 25 36.8115734064	+30 28 21.372380940	263.7	M
RZ Peg	22 05 52.9706535288	+33 30 24.810555528	396.8	M

Table 1. *Cont.*

Target	RA	DEC	Period [1] (Days)	Chemistry
S Peg	23 20 32.6147404416	+08 55 08.162686416	438.7	C
SW Peg	21 22 29.0431372896	+21 59 54.386587176	319.2	M
SX Peg	22 50 24.8246941896	+17 53 36.514618152	396.3	M
V Peg	22 01 02.6126182392	+06 07 11.021504592	303.6	S
Z Peg	00 00 06.5622821352	+25 53 11.249163204	302.4	M
R Per	03 30 03.1202869152	+35 40 16.637728008	201.2	M
Y Per	03 27 42.3911607264	+44 10 36.486741684	209.9	M
S Ser	15 21 39.5340937176	+14 18 53.092200960	248.6	C
S Tau	04 29 11.7453742152	+09 56 43.593074196	371.8	M
V Tau	04 52 02.3036114928	+17 32 16.710466272	374.5	M
S Hya	08 53 33.9475249272	+03 04 06.478567212	168.7	M
S Lac	22 29 00.9084820392	+40 18 55.856923596	256.6	M
V Leo	10 00 01.9201886424	+21 15 44.364417552	241.5	M
Y Lib	15 11 41.3057132755	− 06 00 41.335776376	273.4	M
T Lyn	08 22 42.8487504768	+33 31 09.470511768	275.7	M
RU Lyr	19 12 21.2458817904	+41 18 13.469389632	406	C
RY Lyr	18 44 52.1060974752	+34 40 33.375764640	371.8	M
S Lyr	19 13 11.8046954880	+26 00 27.853438788	325.8	M
U Lyr	19 20 09.1516147560	+37 52 36.919225776	438.4	S
RR Mon	07 17 31.5423447792	+01 05 41.545300920	451.7	C
V Mon	06 22 43.5821819376	− 02 11 43.500924636	394.7	S
RT Oph	17 56 32.0349186096	+11 10 09.696002556	340.5	M
RU Oph	17 32 52.6414079808	+09 25 24.857845212	426.3	M
RY Oph	18 16 36.9362443512	+03 41 35.342410344	202.3	M
SS Oph	16 57 50.9947439640	− 02 45 42.403999500	150.4	M
Z Oph	17 19 32.1158063448	+01 30 54.201255300	180.6	M
R Ori	04 59 00.5594811144	+08 07 49.719678420	348.7	M
R Psc	01 30 38.3144450088	+02 52 53.836476672	377.1	C
S Psc	01 17 34.5467224464	+08 55 52.672154196	344.5	M
X Psc	01 12 07.8095816904	+22 13 24.394877580	404.6	M
R Tri	02 37 02.3403028152	+34 15 51.341675184	349.6	M
RS UMa	12 38 57.5446672272	+58 29 00.194348508	266.9	M
S UMa	12 43 56.6759612760	+61 05 35.501371908	259	M
T UMa	12 36 23.4652834704	+59 29 12.980496552	225.9	S
X UMa	08 40 49.5073410864	+50 08 11.977900116	256.6	M
R Vir	12 38 29.9338039680	+06 59 19.028080356	249	M
RU Vir	12 47 18.4090087128	+04 08 41.356415148	145.6	M
U Vir	12 51 05.7376280088	+05 33 11.548496016	433.2	C
Y Vir	12 33 52.9887378936	− 04 25 19.627433328	206.6	M
			218.4	M

We supplement the interferometric measurements with archival photometric data to determine a target's bolometric flux (F_{bol}) alongside its angular size (θ). Incorporating the target's distance estimate with F_{bol} and θ enables the determination of T_{eff} and $R_{\star}$, respectively. Additionally, the wavelength-dependent characteristics of the narrowband data are utilized to analyze how the relative proportions of molecular features compared to their atmospheric distribution evolve across multiple stellar pulsation cycles; this "map" of the overlying molecular layers will advance our understanding of the time-dependent relationship between the stellar pulsation and the material lofted into the surrounding CSE (see Section 3.2).

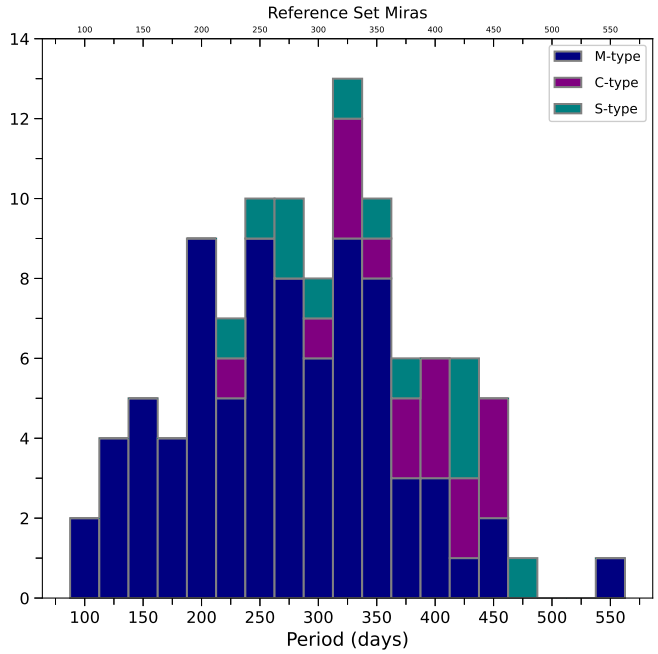


Figure 1. The targets included in our *Mira Reference Dataset* span all 3 chemical sub-classes and an extensive range of periods. Pulsation periods were calculated using the Lomb–Scargle periodogram analysis [43,44] on light curves taken from the American Association of Variable Star Observers (AAVSO). The wide range of periods indicates that our sample includes both fundamental and overtone pulsators.

Typical analysis of Mira and AGB atmospheres relies on building complete atmospheric models, requiring detailed knowledge about chemical abundances, mass loss rates, outflow acceleration, velocities, gas-to-dust ratios, etc., many of which typically have large errors associated with them that will propagate through the models. The detail levels required from observational data to improve these atmospheric models restrict us to the nearest, brightest, and largest targets such as *R Leo* (28–30 mas [45]), *IK Tau* (20 mas [46]), *o Cet* (29–35 mas [47]), etc., and do not allow us to build up statistically significant samples. We use PTI Miras to explore an alternate approach.

Directly measuring and tracking an individual Mira's angular size across different phases allows us to establish a more precise method for determining $R_\star$, T_{eff}, and F_{bol} as functions of time, which can then be utilized alongside complementary data like spectroscopy or distance to directly investigate the CSE (see Figure 2). This approach means that the characterization of each Mira in our PTI set is constrained by the star's unique fundamental characteristics and models can be built from this observational foundation *with minimal assumptions*. For this reason, we refer to this project as developing a *Mira Reference Dataset*, with the PTI dataset at the core, in order to provide those fundamental stellar parameters the community needs. Some PTI Miras also have ancillary data across multiple wavelengths and observational techniques (such as IRAS LRS spectra, Gaia spectroscopy, parallaxes, maser data, etc.). The final website will provide directions to where this additional data can be found for individual targets. Figure 2 conceptualizes how researchers can combine different datasets to characterize the CSE. The full *Mira Reference Dataset* can then be used to support a variety of observational and theoretical studies in pulsation, circumstellar chemistry, and how the interplay between these factors affects dust production in the CSE.

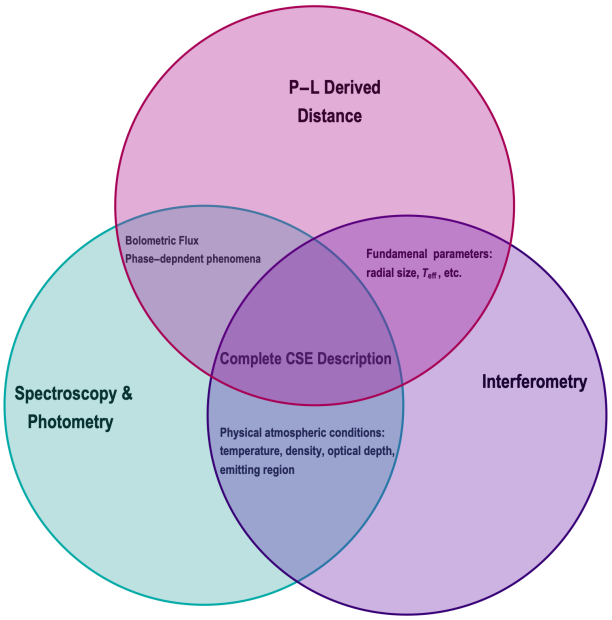


Figure 2. A Venn diagram that conceptualizes our approach to characterizing Mira atmospheres using three distinct measurement/data regions: spectroscopy plus photometry, interferometry, and distance estimates. The overlapping areas show how feedback between these regions enhances our overall understanding of the physical processes involved. At the center, where all three regions overlap, the result is a more comprehensive understanding of the Mira's CSE.

3.1. Case Study I: Spitzer IRS with PTI Wideband Sizes

Infrared spectroscopy is a key diagnostic tool used to study Miras in order to understand their complex molecular atmospheres and trace mass loss processes. A complete understanding of the dynamic and time-dependent nature of dust and molecule production and their relationship to mass loss requires *phase-dependent* efforts.

In 2008, a phase-dependent spectral study was undertaken on a subset of 25 PTI Miras, spanning the O-S-C types with phase. This study utilized Spitzer's IRS at the highest spectral resolutions available (R ∼600) [48,49], over a period of about one year (approximately one pulsation cycle). This experiment was designed to study time-dependent atmospheric spectral signatures and, thus, each target was sampled at 2–7 different phase points, resulting in 96 complete spectra, from 10 to 38 µm. Figure 3 shows an example of Spitzer IRS spectra for the oxygen-rich Mira *S Peg*. This is a uniquely rich dataset, characterized by multiple observations of each star and the high SNR achieved with quick exposure times, all without saturating the detector. These observations were also intentionally taken *simultaneously* with the then-ongoing PTI observations of the same Miras in order to help develop a more complete understanding of the phase relationships and photospheric/temperature/pulsation behaviors of the Mira atmospheres.

The M-types from the Spitzer study show strong unresolved ro–vibrational Q-branch bandheads of CO_2 at 13.87 µm, 14.98 µm, 16.18 µm, with two weaker bandheads at 13.49 µm and 16.76 µm, and a forest of blended, weaker P and R branch transitions (see Figure 3). The three CO_2 Q-branch bandheads at 13.87 µm, 14.98 µm, and 16.18 µm were modeled using the non-local thermodynamic equilibrium (NLTE) radiative transfer code RADEX [50], adapted for use in the mid-IR. This adaptation required a molecular file custom-built for ro–vibrational transitions of CO_2. A complete description of this process can be found in [14,51]. The vibrational energy levels included in the file and a sample slab spectrum calculated with RADEX are provided in Figure 4. The RADEX models provide column density, kinetic temperature, and optical depth. Combining these spectral models with wideband angular diameters measured with PTI and parallax measurements allows us to

directly estimate the emitting region of the CO_2 gas. For specific model results on individual targets, see [14].

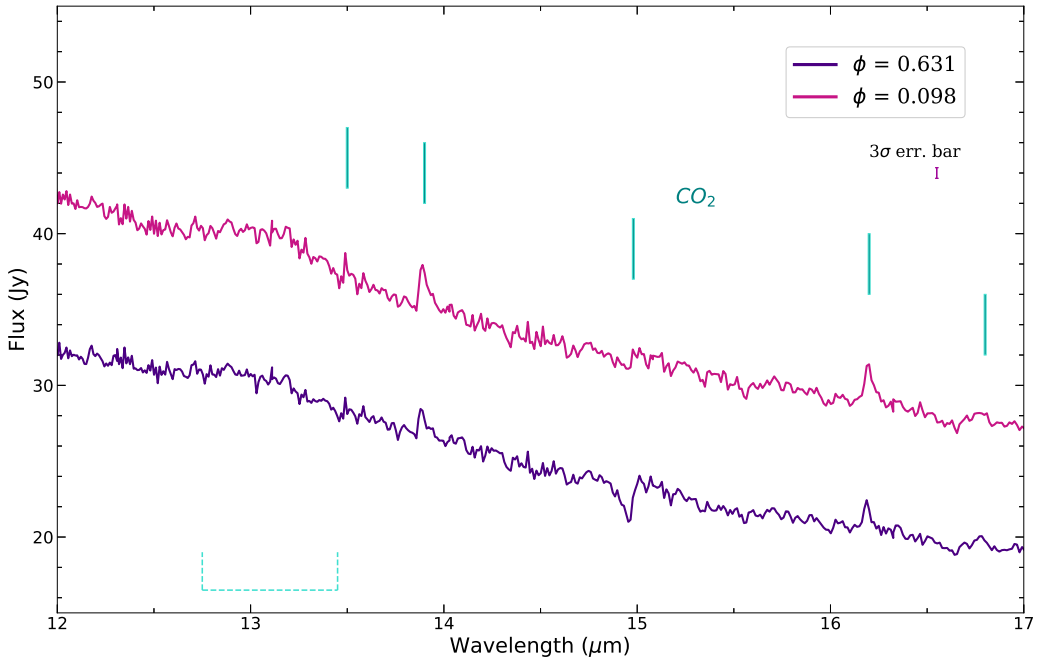


Figure 3. Spitzer IRS spectra of the M-type Mira variable *S Peg*. The top spectrum is artificially offset by 5 Jy for clarity. Note the dramatic change in the 15 μm feature of CO_2 between observations. About half of the M-types in the Spitzer sample also showed the presence of the 13 μm feature.

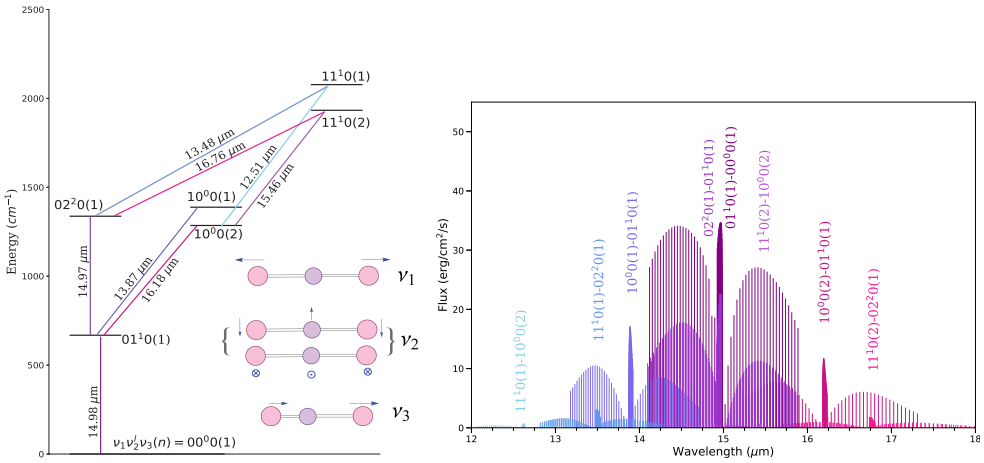


Figure 4. Energy level diagram of CO_2 transitions included in the molecular file with an accompanying sample slab spectrum calculated with RADEX. The vibrational levels and Fermi split levels are labeled according to the HITRAN notation. The colors of the transitions match their respective corresponding bands in the synthetic spectrum [14].

Combining spectral models with interferometric measurements allows us to fully characterize the CO_2 gas without imparting an overabundance of assumptions about individual stars. This more complete understanding of the underlying photospheric behavior and actual physical sizes of the Miras (via distance information) allows us to place the molecular behavior into a more grounded physical context, locating emission and absorption features within the circumstellar atmospheres and identifying when the atmospheres depart from LTE behavior. This type of analysis can be repeated for any of the individual Miras included in the *Reference Dataset* (by this team or others) for which sufficient information exists.

3.2. Case Study II: Narrow-Band PTI Atmospheric Layers of S Lac

One intriguing aspect of the PTI observations, which directly impacts the determination of pulsation modes for these stars, concerns the following: *what are the spectro-interferometric measurements actually 'seeing'?* The narrow-band data show the same wavelength-dependent sizes described in Section 2. Since the (low-resolution) spectral signatures seen in these Miras are related to molecular features in the CSE, the varying opacity as a function of wavelength effectively means that the narrow-band channels are probing different molecular layers within the atmosphere (see Figure 5). We expect the morphology of these layers to evolve across the stellar pulsation cycle. Studies using the Very Large Telescope Interferometer (VLTI) in Chile have attempted to tease out some of these details [52–54], but rarely followed more than a few Miras for even one complete pulsation cycle. Exploring the time-dependent behavior of these molecular layers in relation to each other is expected to reveal the dynamic relationship between stellar pulsation and the surrounding atmosphere.

For example, the preliminary narrowband analysis of the M-type *S Lac* (provided in Figure 5) shows three layers: a continuum at 2.2 µm, an H_2O layer at 2.0 µm, and a CO layer at 2.4 µm. The angular diameter sizes represent averages of the wrapped-phase sizes that were binned by 0.1 phase, with each bin including at least five measurements. The angular diameter of the continuum is the smallest between phase 0.9 and 0.1 and the largest at phase 0.6, which agrees well with the pulsating photosphere acting as a mechanical piston. (Note: "phase" values here correspond to the optical light curve, with phase 0 occurring at maximum optical light and phase 0.5 near minimum optical light.) But we notice that the H_2O and CO layers are actually the most extended at phase 0.3, and then drop back and track the underlying continuum layer's behavior from phase 0.4 to 0.9. This sharp increase in the molecular layers' angular diameters could potentially indicate that as the pulsation shock moved through the atmosphere, it mechanically lofted these layers. We will perform a similar narrowband analysis on the remaining Miras to continue studying the relationships between the photosphere, surrounding molecular layers, and stellar pulsation.

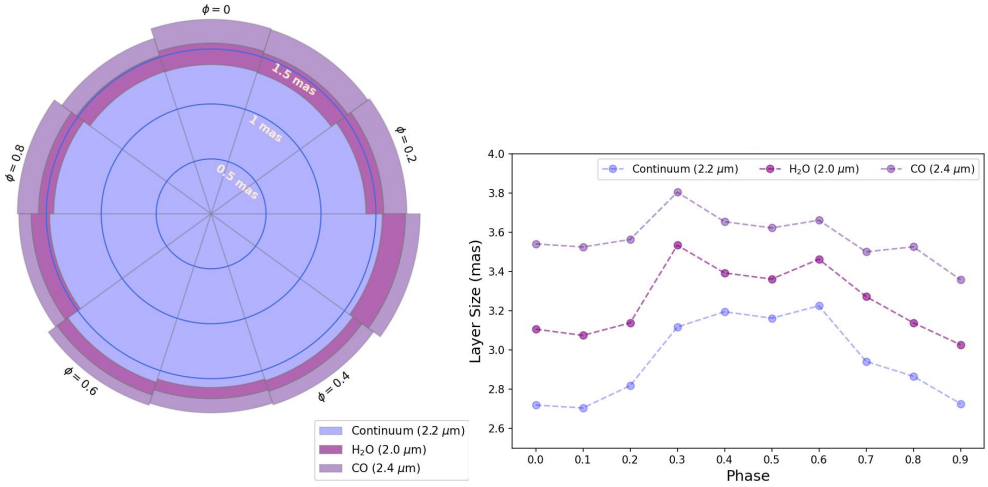


Figure 5. Two different ways to visualize the PTI narrowband angular sizes with the phase for the M-type Mira *S Lac*. The left insert (which visually resembles a layered tart) displays the angular diameters as wedges with the phase increasing in a clockwise direction. The circles increase radially from 0.5 to 1.5 mas for scale. Tracing the layers through a pulsation cycle in this manner provides more physical context to the visualization, which can be difficult for non-interferometry experts to see in standard size vs phase plots. The right insert displays the same data as conventional sizes vs. the phase plot. The angular sizes were binned by the 0.1 phase and each bin includes at least 5 measurements. The 3 layers correspond to the narrowband continuum (2.2 µm), H_2O (2.0 µm), and CO (2.4 µm) measurements. These narrowband data let us track how the photosphere and the surrounding H_2O and CO layers respond to the pulsation.

4. Collaboration

Our *Mira Reference Dataset* project has multiple exciting collaboration opportunities with both the professional and citizen science communities. The project will benefit greatly from contributions from citizen science observing associations, such as the Association Française des Observateurs d'Étoiles Variables (AFOEV) and the American Association of Variable Star Observers (AAVSO). (Note: these are just two examples in an international list of available associations.) In particular, regular multi-wavelength monitoring across multiple pulsation cycles is fundamental for studies of variable stars because well-sampled light curves can reveal anomalies, such as dimming events, double-pulsations, or period switching, and these are absolutely crucial to our understanding of how these stars are evolving. This type of detailed, long-term monitoring is difficult at professional large-aperture telescope facilities, which require TAC-approved proposals for ∼hours to days that typically must be re-submitted two or more times per year. Contributions from the citizen science astronomical community on these targets will enhance this Mira *Mira Reference Dataset*, and make it all the more valuable for the community of observers, theorists, and modelers who care about the types of questions that Miras are well-posed to help answer.

As the astrophysical community includes more time-domain and multi-messenger programs to achieve science goals outlined in the latest Decadal survey [55], we will likely see an increase in variable star studies and observations. Our team is open to (and eager for) further scientific collaboration on any of these targets. We are currently in the final stages of publishing the *Mira Reference Dataset* website for easy access to these targets. The website is designed for users to look up any target of interest from the PTI set and find the PTI measurements as well as the location for any ancillary data on that particular target. For teams currently working on (or planning new) observations of Miras, please consider corresponding with us about including targets from the *Mira Reference Dataset*.

5. Conclusions

Mira variables serve as excellent laboratories for studying a variety of astrophysical phenomena. By utilizing interferometric techniques, a new era of high-precision experiments can be conducted. We will use 10 years of near-IR interferometric monitoring data as the foundation to build our wonderful *Mira Reference Dataset* for the community to utilize. This dataset can be supplemented with multi-wavelength and multi-messenger observations from both professional and citizen scientists. Together, we will develop an unprecedented, detailed description of the physical properties of Miras and their surrounding CSEs as we advance our understanding of these truly wonderful stars.

Author Contributions: Conceptualization, D.K.B.-A., M.J.C.-E., and G.T.v.B.; methodology, D.K.B.-A., M.J.C.-E., G.T.v.B., G.T.v.B., M.J.C.-E., and D.K.B.-A.; validation, G.T.v.B., M.J.C.-E., and D.K.B.-A.; formal analysis, D.K.B.-A., M.J.C.-E., and G.T.v.B.; investigation, D.K.B.-A., M.J.C.-E., and G.T.v.B.; resources, G.T.v.B. and M.J.C.-E.; data curation, G.T.v.B., M.J.C.-E., and D.K.B.-A.; writing—original draft preparation, D.K.B.-A.; writing—review and editing, D.K.B.-A. and M.J.C.-E.; visualization, D.K.B.-A., M.J.C.-E., and G.T.v.B.; supervision, M.J.C.-E. and G.T.v.B.; project administration, M.J.C.-E. and G.T.v.B.; funding acquisition, M.J.C.-E. and G.T.v.B. All authors have read and agreed to the published version of the manuscript.

Funding: This work is currently being supported through the National Science Foundation under grant number 2206803. The Spitzer study was originally supported through a NASA Spitzer grant for Program GO 50717, funded through NASA-JPL under contract 1344355. This work is based [in part] on observations made with the Spitzer Space Telescope, which was operated by the Jet Propulsion Laboratory, California Institute of Technology under a contract with NASA. Science operations with PTI were conducted through the efforts of the PTI Collaboration (https://nexsci.caltech.edu/missions/Palomar/ (28 October 2024), and we acknowledge the invaluable contributions of our PTI colleagues. Funding for PTI was provided to the Jet Propulsion Laboratory under its TOPS (Towards Other Planetary Systems), ASEPS (Astronomical Studies of Extrasolar Planetary Systems), and Origins programs and from the JPL Director's Discretionary Fund. Portions of this work were

performed at the Jet Propulsion Laboratory, California Institute of Technology, under contract with the National Aeronautics and Space Administration.

Data Availability Statement: We are in the final stages of publishing the *Mira Reference Dataset* website, which will be hosted at Lowell Observatory. Data produced for this investigation will be made available at the NASA Exoplanet Science Institute (NExScI) PTI archive (https://nexsci.caltech.edu/software/PTISupport/ (28 October 2024).

Acknowledgments: The authors would like to thank the organizing committee of the XIV Torino Workshop on AGB Stars for including our work in this meeting and in the proceedings. The authors wish to acknowledge the variable star observations from the AAVSO International Database (contributed to by observers worldwide and used in this research effort). We have made extensive use of the SIMBAD database [56] and the VizieR catalog access tool, operated by the CDS in Strasbourg, France [57].

Conflicts of Interest: The authors declare no conflicts of interest.

Abbreviations

The following abbreviations are used in this manuscript:

AGB	asymptotic giant branch
CSE	circumstellar environment
PTI	Palomar Testbed Interferometer
ISI	Infrared Spatial Interferometer
IOTA	Infrared Optical Telescope Array
VLTI	Very Large Telescope Interferometer
AFOEV	Association Française des Observateurs d'Étoiles Variables
AAVSO	American Association of Variable Star Observers
ISM	interstellar medium

References

1. Freytag, B.; Liljegren, S.; Höfner, S. Global 3D radiation-hydrodynamics models of AGB stars. Effects of convection and radial pulsations on atmospheric structures. *Astron. Astrophys.* **2017**, *600*, A137. [CrossRef]
2. Valiante, R.; Schneider, R.; Bianchi, S.; Andersen, A.C. Stellar sources of dust in the high-redshift Universe. *Mon. Not. R. Astron. Soc.* **2009**, *397*, 1661–1671. [CrossRef]
3. Prager, H.A.; Willson, L.A.; Marengo, M.; Creech-Eakman, M.J. Relation of Observable Stellar Parameters to Mass-loss Rate of AGB Stars in the LMC. *Astrophys. J.* **2022**, *941*, 44. [CrossRef]
4. Decin, L. Evolution and Mass Loss of Cool Ageing Stars: A Daedalean Story. *Annu. Rev. Astron. Astrophys.* **2021**, *59*, 337–389. [CrossRef]
5. Van de Sande, M. Chemical complexity and dust formation around evolved stars. *arXiv* **2024**, arXiv:2408.08153.
6. van Belle, G.T.; Dyck, H.M.; Thompson, R.R.; Benson, J.A.; Kannappan, S.J. Angular Size Measurements of Carbon Miras and S-Type Stars. *Astron. J.* **1997**, *114*, 2150. [CrossRef]
7. Herwig, F. Evolution of Asymptotic Giant Branch Stars. *Annu. Rev. Astron. Astrophys.* **2005**, *43*, 435–479. [CrossRef]
8. Cherchneff, I. A chemical study of the inner winds of asymptotic giant branch stars. *Astron. Astrophys.* **2006**, *456*, 1001–1012. [CrossRef]
9. Danilovich, T.; Bergman, P.; Justtanont, K.; Lombaert, R.; Maercker, M.; Olofsson, H.; Ramstedt, S.; Royer, P. Detailed modelling of the circumstellar molecular line emission of the S-type AGB star W Aquilae. *Astron. Astrophys.* **2014**, *569*, A76. [CrossRef]
10. Höfner, S.; Olofsson, H. Mass loss of stars on the asymptotic giant branch. Mechanisms, models and measurements. *Astron. Astrophys. Rev.* **2018**, *26*, 1. [CrossRef]
11. Buss, R.H., Jr.; Tielens, A.G.G.M.; Cohen, M.; Werner, M.W.; Bregman, J.D.; Witteborn, F.C. Infrared Spectra of Transition Objects and the Composition and Evolution of Carbon Dust. *Astrophys. J.* **1993**, *415*, 250. [CrossRef]
12. Sloan, G.C.; Lagadec, E.; Zijlstra, A.A.; Kraemer, K.E.; Weis, A.P.; Matsuura, M.; Volk, K.; Peeters, E.; Duley, W.W.; Cami, J.; et al. Carbon-rich Dust Past the Asymptotic Giant Branch: Aliphatics, Aromatics, and Fullerenes in the Magellanic Clouds. *Astrophys. J.* **2014**, *791*, 28. [CrossRef]
13. Höfner, S. A new generation of dynamic model atmospheres for AGB stars: First results. *Astron. Astrophys.* **1999**, *346*, L9–L12.
14. Baylis-Aguirre, D.K. A Mid-Infrared Study of Mira Variable Atmospheres: Phase Dependent Analysis of Spectral Lines Observed with the Spitzer IRS. Ph.D. Thesis, New Mexico Institute of Mining and Technology, Socorro, NM, USA, 2021.
15. van Leeuwen, F. Validation of the new Hipparcos reduction. *Astron. Astrophys.* **2007**, *474*, 653–664. [CrossRef]
16. Gaia Collaboration. VizieR Online Data Catalog: Gaia DR2 (Gaia Collaboration, 2018). *VizieR Online Data Catalog.* **2018**. [CrossRef]

17. van Belle, G.T.; Thompson, R.R.; Creech-Eakman, M.J. Angular Size Measurements of Mira Variable Stars at 2.2 Microns. II . *Astron. J.* **2002**, *124*, 1706–1715. [CrossRef]
18. Thompson, R.R.; Creech-Eakman, M.J.; van Belle, G.T. Multiepoch Interferometric Study of Mira Variables. I. Narrowband Diameters of RZ Pegasi and S Lacertae . *Astrophys. J.* **2002**, *577*, 447–456. [CrossRef]
19. Zhang, H.; Sanders, J.L. A kinematic calibration of the O-rich Mira variable period-age relation from Gaia. *Mon. Not. R. Astron. Soc.* **2023**, *521*, 1462–1478. [CrossRef]
20. Rowell, N.; Davidson, M.; Lindegren, L.; van Leeuwen, F.; Castañeda, J.; Fabricius, C.; Bastian, U.; Hambly, N.C.; Hernández, J.; Bombrun, A.; et al. Gaia Early Data Release 3. Modelling and calibration of Gaia's point and line spread functions. *Astron. Astrophys.* **2021**, *649*, A11. [CrossRef]
21. Pourbaix, D.; Platais, I.; Detournay, S.; Jorissen, A.; Knapp, G.; Makarov, V.V. How many Hipparcos Variability-Induced Movers are genuine binaries? *Astron. Astrophys.* **2003**, *399*, 1167–1175. [CrossRef]
22. Chiavassa, A.; Pasquato, E.; Jorissen, A.; Sacuto, S.; Babusiaux, C.; Freytag, B.; Ludwig, H.G.; Cruzalèbes, P.; Rabbia, Y.; Spang, A.; et al. Radiative hydrodynamic simulations of red supergiant stars. III. Spectro-photocentric variability, photometric variability, and consequences on Gaia measurements. *Astron. Astrophys.* **2011**, *528*, A120. [CrossRef]
23. Chiavassa, A.; Freytag, B.; Schultheis, M. Heading Gaia to measure atmospheric dynamics in AGB stars. *Astron. Astrophys.* **2018**, *617*, L1. [CrossRef]
24. Glass, I.S.; Evans, T.L. A period-luminosity relation for Mira variables in the Large Magellanic Cloud . *Nature* **1981**, *291*, 303–304. [CrossRef]
25. Feast, M.W.; Glass, I.S.; Whitelock, P.A.; Catchpole, R.M. A period-luminosity-colour relation for Mira variables. *Mon. Not. R. Astron. Soc.* **1989**, *241*, 375–392. [CrossRef]
26. Nowotny, W.; Kerschbaum, F.; Olofsson, H.; Schwarz, H.E. A census of AGB stars in Local Group galaxies. II. NGC 185 and NGC 147. *Astron. Astrophys.* **2003**, *403*, 93–103. [CrossRef]
27. Feast, M.W. The Ages, Masses, Evolution and Kinematics of Mira Variables. *arXiv* **2009**, arXiv:0812.0250 48–53. [CrossRef]
28. Sun, Y.; Zhang, J.; Zhang, B.; Xu, S.; Mai, X.; Ding, H.; Chen, W.; Wen, S. Miras as a distance indicator in the CSST, JWST, and Gaia era. *Front. Astron. Space Sci.* **2023**, *10*, 1232151. [CrossRef]
29. Feast, M.; Whitelock, P.A. Variable Stars and Galactic Structure. In *Proceedings of the International Astronomical Union* ; Feltzing, S., Zhao, G., Walton, N.A., Whitelock, P., Eds.; Cambridge University Press: Cambridge, UK, 2014; Volume 298, pp. 40–52. [CrossRef]
30. Wood, P.R. The pulsation modes, masses and evolution of luminous red giants. *Mon. Not. R. Astron. Soc.* **2015**, *448*, 3829–3843. [CrossRef]
31. Whitelock, P.A.; Feast, M.W.; Van Leeuwen, F. AGB variables and the Mira period-luminosity relation. *Mon. Not. R. Astron. Soc.* **2008**, *386*, 313–323. [CrossRef]
32. Feast, M.; Whitelock, P.; Menzies, J. Globular clusters and the Mira period-luminosity relation. *Mon. Not. R. Astron. Soc.* **2002**, *329*, L7–L12. [CrossRef]
33. Willson, L.A.; Marengo, M. Miras. *J. Am. Assoc. Var. Star Obs.* **2012**, *40*, 516–527. Available online: https://ui.adsabs.harvard.edu/abs/2012JAVSO..40..516W (accessed on 28 October 2024).
34. Sutton, E.C.; Storey, J.W.V.; Betz, A.L.; Townes, C.H.; Spears, D.L. Spatial heterodyne interferometry of VY Canis Majoris, Alpha Orionis, Alpha Scorpii, and R Leonis at 11 microns. *Astrophys. J.* **1977**, *217*, L97–L100. [CrossRef]
35. Tatebe, K.; Chandler, A.A.; Hale, D.D.S.; Townes, C.H. Characterization of Dust Shell Dynamics and Asymmetry for Six Mira-Type Stars. *Astrophys. J.* **2006**, *652*, 666–680. [CrossRef]
36. van Belle, G.T.; Dyck, H.M.; Benson, J.A.; Lacasse, M.G. Angular Size Measurements of 18 Mira Variable Stars at 2.2 microns. *Astron. J.* **1996**, *112*, 2147. [CrossRef]
37. Ragland, S.; Traub, W.A.; Berger, J.P.; Danchi, W.C.; Monnier, J.D.; Willson, L.A.; Carleton, N.P.; Lacasse, M.G.; Millan-Gabet, R.; Pedretti, E.; et al. First Surface-resolved Results with the Infrared Optical Telescope Array Imaging Interferometer: Detection of Asymmetries in Asymptotic Giant Branch Stars. *Astrophys. J.* **2006**, *652*, 650–660. [CrossRef]
38. van Belle, G.T.; Paladini, C.; Aringer, B.; Hron, J.; Ciardi, D. The PTI Carbon Star Angular Size Survey: Effective Temperatures and Non-sphericity. *Astrophys. J.* **2013**, *775*, 45. [CrossRef]
39. Millan-Gabet, R.; Pedretti, E.; Monnier, J.D.; Schloerb, F.P.; Traub, W.A.; Carleton, N.P.; Lacasse, M.G.; Segransan, D. Diameters of Mira Stars Measured Simultaneously in the J, H, and K' Near-Infrared Bands. *Astrophys. J.* **2005**, *620*, 961–969. [CrossRef]
40. Lançon, A.; Wood, P.R. A library of 0.5 to 2.5 mu m spectra of luminous cool stars. *Astron. Astrophys. Suppl. Ser.* **2000**, *146*, 217–249. [CrossRef]
41. Colavita, M.M.; Wallace, J.K.; Hines, B.E.; Gursel, Y.; Malbet, F.; Palmer, D.L.; Pan, X.P.; Shao, M.; Yu, J.W.; Boden, A.F.; et al. The Palomar Testbed Interferometer. *Astrophys. J.* **1999**, *510*, 505–521. [CrossRef]
42. Samus', N.N.; Kazarovets, E.V.; Durlevich, O.V.; Kireeva, N.N.; Pastukhova, E.N. General catalogue of variable stars: Version GCVS 5.1. *Astron. Rep.* **2017**, *61*, 80–88. [CrossRef]
43. Lomb, N.R. Least-Squares Frequency Analysis of Unequally Spaced Data. *Astrophys. Space Sci.* **1976**, *39*, 447–462. [CrossRef]
44. Scargle, J.D. Studies in astronomical time series analysis. II-Statistical aspects of spectral analysis of unevenly spaced data. *Astrophys. J.* **1982**, *263*, 835–853. [CrossRef]

45. Perrin, G.; Coudé du Foresto, V.; Ridgway, S.T.; Mennesson, B.; Ruilier, C.; Mariotti, J.M.; Traub, W.A.; Lacasse, M.G. Interferometric observations of R Leonis in the K band. First direct detection of the photospheric pulsation and study of the atmospheric intensity distribution. *Astron. Astrophys.* **1999**, *345*, 221–232.
46. Monnier, J.D.; Millan-Gabet, R.; Tuthill, P.G.; Traub, W.A.; Carleton, N.P.; Coudé du Foresto, V.; Danchi, W.C.; Lacasse, M.G.; Morel, S.; Perrin, G.; et al. High-Resolution Imaging of Dust Shells by Using Keck Aperture Masking and the IOTA Interferometer. *Astrophys. J.* **2004**, *605*, 436–461. [CrossRef]
47. Woodruff, H.C.; Eberhardt, M.; Driebe, T.; Hofmann, K.H.; Ohnaka, K.; Richichi, A.; Schertl, D.; Schöller, M.; Scholz, M.; Weigelt, G.; et al. Interferometric observations of the Mira star o Ceti with the VLTI/VINCI instrument in the near-infrared. *Astron. Astrophys.* **2004**, *421*, 703–714. [CrossRef]
48. Creech-Eakman, M.J.; Güth, T.; Luttermoser, D.G.; Jurgenson, C.A.; Speck, A.K. An Interferometrically Derived Sample of Miras with Phase using Spitzer: Paper I - A First Look. *Astron. Rev.* **2012**, *7*, 4–24. [CrossRef]
49. Creech-Eakman, M.; Hora, J.; Ivezic, Z.; Jurgenson, C.; Luttermoser, D.; Marengo, M.; Stencel, R.; Thompson, R. An Interferometric Snapshot Survey to Constrain Mass-Loss Dynamics and Physics in AGB Stars. *Spitzer Proposals, 50717* 2008. Available online: https://ui.adsabs.harvard.edu/abs/2008sptz.prop50717C (accessed on 28 October 2024).
50. van der Tak, F.F.S.; Black, J.H.; Schöier, F.L.; Jansen, D.J.; van Dishoeck, E.F. A computer program for fast non-LTE analysis of interstellar line spectra. With diagnostic plots to interpret observed line intensity ratios. *Astron. Astrophys.* **2007**, *468*, 627–635. [CrossRef]
51. Baylis-Aguirre, D.K.; Creech-Eakman, M.J.; Güth, T. Mid-IR spectra of the M-type Mira variable R Tri observed with the Spitzer IRS. *Mon. Not. R. Astron. Soc.* **2020**, *493*, 807–814. [CrossRef]
52. Haubois, X.; Wittkowski, M.; Perrin, G.; Kervella, P.; Mérand, A.; Thiébaut, E.; Ridgway, S.T.; Ireland , M.; Scholz, M. Resolving asymmetries along the pulsation cycle of the Mira star X Hydrae. *Astron. Astrophys.* **2015**, *582*, A71. [CrossRef]
53. Zhao-Geisler, R.; Köhler, R.; Kemper, F.; Kerschbaum, F.; Mayer, A.; Quirrenbach, A.; Lopez, B. Spectro-Imaging of the Asymmetric Inner Molecular and Dust Shell Region of the Mira Variable W Hya with MIDI/VLTI. *Publ. Astron. Soc. Pac.* **2015**, *127*, 732. [CrossRef]
54. Wittkowski, M.; Rau, G.; Chiavassa, A.; Höfner, S.; Scholz, M.; Wood, P.R.; de Wit, W.J.; Eisenhauer, F.; Haubois, X.; Paumard, T. VLTI-GRAVITY measurements of cool evolved stars. I. Variable photosphere and extended atmosphere of the Mira star R Peg. *Astron. Astrophys.* **2018**, *613*, L7. [CrossRef]
55. National Academies of Sciences, Engineering, and Medicine. *Consenses Study Report. National Academies of Sciences, Engineering, and Medicine*; National Academies: Washington, DC, USA, 2021. [CrossRef]
56. Wenger, M.; Ochsenbein, F.; Egret, D.; Dubois, P.; Bonnarel, F.; Borde, S.; Genova, F.; Jasniewicz, G.; Laloë, S.; Lesteven, S.; et al. The SIMBAD astronomical database. The CDS reference database for astronomical objects. *Astron. Astrophys. Suppl. Ser.* **2000**, *143*, 9–22. [CrossRef]
57. Ochsenbein, F.; Bauer, P.; Marcout, J. The VizieR database of astronomical catalogues. *Astron. Astrophys. Suppl. Ser.* **2000**, *143*, 23–32. [CrossRef]

Disclaimer/Publisher's Note: The statements, opinions and data contained in all publications are solely those of the individual author(s) and contributor(s) and not of MDPI and/or the editor(s). MDPI and/or the editor(s) disclaim responsibility for any injury to people or property resulting from any ideas, methods, instructions or products referred to in the content.